Available online at www.sciencedirect.com
ScienceDirect
Solid State Ionics 179 (2008) 565–573
SOLID STATE IONICS
www.elsevier.com/locate/ssi

High density flip-flop hydrogen-bonding networks in the β-cyclodextrin heptaiodide inclusion complexes with Bi^{3+} and Te^{4+} ions. Combined dielectric relaxation, Raman scattering and thermal analysis

Vasileios G. Charalampopoulos, John C. Papaioannou *

Laboratory of Physical Chemistry, Department of Chemistry, National and Kapodistrian University of Athens P.O. BOX 64004, 157 10 Zografou, Athens, Greece

Received 23 January 2008; received in revised form 14 March 2008; accepted 4 April 2008

Abstract

The polycrystalline inclusion complexes $(\beta\text{-CD})_2\cdot TeI_7\cdot 17H_2O$ and $(\beta\text{-CD})_2\cdot BiI_7\cdot 17H_2O$ have been investigated via dielectric spectroscopy over a frequency range of 0–100 kHz and the temperature range of 140–425 K. Furthermore, a DSC study was carried out in the range of 273–423 K, whereas the Raman spectra (303–393 K) of β-Te were compared to the previously examined ones of β-Bi. In the case of β-Te an important percentage of normal H-bonds is transformed into flip-flop ones (T_{trans}=216.8 K) as it comes out by the corresponding ε' (T), ε'' (T) and $\varphi(T)$ variations at T<250 K ($\Delta\varepsilon'$=18.6, ε''_{max}=4.8, φ_{min}=69.9°). In β-Bi the greatest percentage of normal H-bonds is transformed into those of the flip-flop type (T_{trans}=223.6 K, $\Delta\varepsilon'$=49.6, ε''_{max}=16, φ_{min}=58.6°) producing a disordered H-bonding network of a much higher density than that of β-Te. At T>250 K, the ac-conductivity ($\ln\sigma$ *vs.* $1/T$) of these systems follows an Arrhenius behaviour with activation energies 0.54 and 0.46 eV for β-Te and 0.38, 0.68 and 0.58 eV for β-Bi. This exponential increment reflects the combined contributions of the water network, the oscillating cations and the dehydration process. The abrupt increase of the ac-conductivity at T>398.5 K is caused by the sublimation of iodine. The temperature-dependent Raman spectra of β-Te exhibit the band shift of 178→172 cm^{-1} which is identical to that of β-Bi, implying a similar elongation of their I_2 units. The high density flip-flop hydrogen-bonding network in the latter complex seems to play a key role in limiting the Lewis base character of I^-_3.

Keywords: β-cyclodextrin; Heptaiodide ions; Dielectric spectroscopy; Raman spectroscopy; Order–disorder

1. Introduction

Flip-flop hydrogen bonds O–(1/2H)···(1/2H)–O are characterized by the existence of H-atoms that are dynamically disordered in two energetically near-equivalent positions, presenting similar occupational parameters (~0.5). This entropically favored hydrogen-bonding scheme has been detected in the crystals of hydrated β-cyclodextrin (β-CD) systems at room temperature, by means of neutron-diffraction analysis [1–3]. More specifically, endless chains and circular arrangements of flip-flop type were observed, consisting of β-CD hydroxyl groups as well as disordered (distributed over specific positions) water molecules. The detailed determination of the crystal structure of $\beta\text{-CD}\cdot 11D_2O$ at 120 K [4], revealed that almost all of the flip-flop hydrogen bonds had been transformed into normal ones O–H···O–H (disorder–order transition). This experimental result verified that the nature of the aforementioned disorder was dynamic, something that had been preliminary indicated via the calorimetric study of $\beta\text{-CD}\cdot 11H_2O$ (ordering of the disordered H-bonds at 227 K during cooling) [5].

Apart from the techniques described above, dielectric spectroscopy has proven to be an excellent tool for the detection of the disorder phenomena in the crystalline β-CD compounds. More specifically, we have carried out dielectric measurements (0–100 kHz) of dried and non-dried samples of β-CD and β-CD with 4-t-butylbenzyl alcohol in the temperature range of

* Corresponding author. Fax: +30 210 7274752.
E-mail address: jpapaioannou@chem.uoa.gr (J.C. Papaioannou).

0167-2738/$ - see front matter © 2008 Elsevier B.V. All rights reserved.
doi:10.1016/j.ssi.2008.04.003

130–350 K [6]. The transition of the normal H-bonds to those of the flip-flop type (order–disorder) was depicted in the $\varepsilon'(T)$ and $\varepsilon''(T)$ variations as a sigmoid fashion and a bell-shaped curve, respectively. Additionally, an important contribution of the water network to the proton conduction was observed, as the temperature was raised. Therefore, we were motivated to expand our studies to a series of β-CD polyiodide inclusion complexes with various metal ions (named β-M, M stands for the corresponding metal). Regardless of the metal ion's nature all of them are isomorphous to β-K (monoclinic $P2_1$) whose single crystal structure has been determined in detail by means of X-ray analysis [7]. According to this work, the β-CD molecules are arranged head to head producing dimers which form parallel cylinders and enclose zigzagged polyiodide chains. Each polyiodide chain consists of discrete and Z-shaped heptaiodide ions which can be formulated as $I_2 \cdot I^-_3 \cdot I_2$. The two disordered I_2 units are included in the β-CD cavities, whereas the central and well-ordered I^-_3 unit is located between the neighboring dimers. The M^{n+} ions are also located between the dimers (but outside the β-CD cylinders) interacting with the β-CD hydroxyls and the water molecules of the interstices.

The dielectric investigation of β-Ba, β-Cd, β-Li, β-K and β-Cs complexes in the temperature range of 140–420 K [8–11], revealed the order–disorder transition of some normal H-bonds to those of the flip-flop type at ~200 K along with the existence of two kinds of water molecules in the crystal lattice (tightly bound and easily movable). Above ~290 K the ac-conductivity presented an Arrhenius exponential increment (linear part in the $\ln\sigma(1/T)$ plot) due to the continuous transformation $(H_2O)_{\text{tightly bound}} \rightarrow (H_2O)_{\text{easily movable}}$ and the contribution of the metal ions' oscillations. During the dehydration process deviations from the Arrhenius behaviour were observed (lower increasing rate) as a consequence of the progressive removal of the water molecules which resulted in the gradual breakdown of the water network. The rapid increase of (σ) at ~403 K was caused by the sublimation of iodine which provided conduction paths [12] between the neighboring I^-_7 ions. The above results were in agreement with those obtained from differential scanning calorimetry. The double endothermic peaks in the range of 343–398 K were directly related to the fractions of the easily movable and tightly bound water molecules. The appearance of a third peak at 403–408 K confirmed the sublimation of iodine.

Furthermore, the above inclusion complexes as well as the β-Na, β-Rb, β-Sr, β-Bi and β-V have been examined via Raman spectroscopy in the temperature range of 303–423 K [8–11,13] and valuable information was gathered about the heptaiodide structural changes. All of these systems presented a transformation of the disordered I_2 units into well-ordered ones (disorder–order transition) as the temperature was raised. This procedure resulted in an elongation of the intraiodine distances d(I–I) whose values were estimated according to the empirical correlation ν(I–I) − d(I–I) for weak-medium strength charge-transfer compounds, suggested by Deplano et al. [14,15]. At room temperature, each spectrum exhibited a strong band at the common frequency of 178–179 cm^{-1} (d(I–I) = ~2.72 Å) which was associated with the ν_1 mode of the disordered iodine molecules. During heating the β-Cs, β-Rb, β-K, β-Na and β-Ba complexes displayed a gradual shift of the initial band to the final single frequency of 165–166 cm^{-1} (d(I–I) = 2.77 Å). In the case of β-Sr and β-Bi complexes the initial Raman band (178 cm^{-1}) was gradually shifted to the final single frequency of 170 (d(I–I) = 2.75 Å) and 172 cm^{-1} (2.72 Å < d(I–I) < 2.75 Å), respectively. The existence of a single band at high temperatures indicated that in each system the two I_2 units of I^-_7 presented an equal I–I elongation due to a symmetric charge-transfer interaction $I_2 \leftarrow I^-_3 \rightarrow I_2$. On the contrary, the β-Li, β-Cd and β-V complexes exhibited a shift of their initial band (178 cm^{-1}) to a double band of frequencies 168, 165 cm^{-1}, 170, 165 cm^{-1} and 173, 165 cm^{-1}, respectively. The two coexistent bands at elevated temperatures implied that the two I_2 molecules of each heptaiodide presented a different I–I elongation as a result of a non-symmetric charge-transfer interaction $I_2 \leftarrow I^-_3 \longrightarrow I_2$.

These spectral data were explained by taking into consideration the metal–triiodide interactions which are determined by the ionic potential q/r of the metals [16] and their position relative to I^-_3. Thus, we have drawn the following general conclusions:

I. When the ionic potential of the cations is lower than ~1.50 (Cs^+, Rb^+, K^+, Na^+ and Ba^{2+}) the $M^{n+\cdots}$ I^-_3 interactions are negligible and the symmetric charge-transfer interaction $I_2 \leftarrow I^-_3 \rightarrow I_2$ remains unaffected (178–179 → 165–166 cm^{-1}).

II. Cations with an ionic potential that is greater than ~1.50 (Li^+, Sr^{2+}, Cd^{2+}, Bi^{3+} and V^{3+}) exhibit significant interactions with the I^-_3 ion. In the case of a face-on position of the metal (Sr^{2+}, Bi^{3+}) relative to I^-_3 the symmetric charge-transfer interaction $I_2 \leftarrow I^-_3 \rightarrow I_2$ is attenuated (Fig. 1a). When the metal (Li^+, Cd^{2+}, V^{3+}) presents a side-on position relative to I^-_3 the charge-transfer interaction becomes non-symmetric $I_2 \leftarrow I^-_3 \longrightarrow I_2$ (Fig. 1b).

In the present paper a dielectric spectroscopy study of β-Te and β-Bi complexes is carried out in a frequency range of 0–100 kHz and in the temperature range of 140–425 K. Additionally, the Raman spectrum of β-Te is examined in the temperature range of 303–393 K and calorimetric measurements of β-Te and β-Bi are accomplished in the temperature range of 273–423 K.

2. Experimental

β-Cyclodextrin, iodine and tellurium iodide (TeI_4) were purchased from Alfa Aesar and bismuth iodide (BiI_3) was purchased from Aldrich. For the preparation of β-Te, 1 g of β-CD was dissolved in 80 mL of distilled water at room temperature under stirring, until the solution became almost saturated. Then 0.36 g of tellurium iodide and 0.44 g solid iodine were simultaneously added to the solution and it was heated to 70 °C for 20–25 min. The hot solution was transferred quickly through a folded filter to an empty beaker (100 mL) which was covered with Teflon and then immersed in a Dewar flask (500 mL) containing hot water (~70 °C). After two days

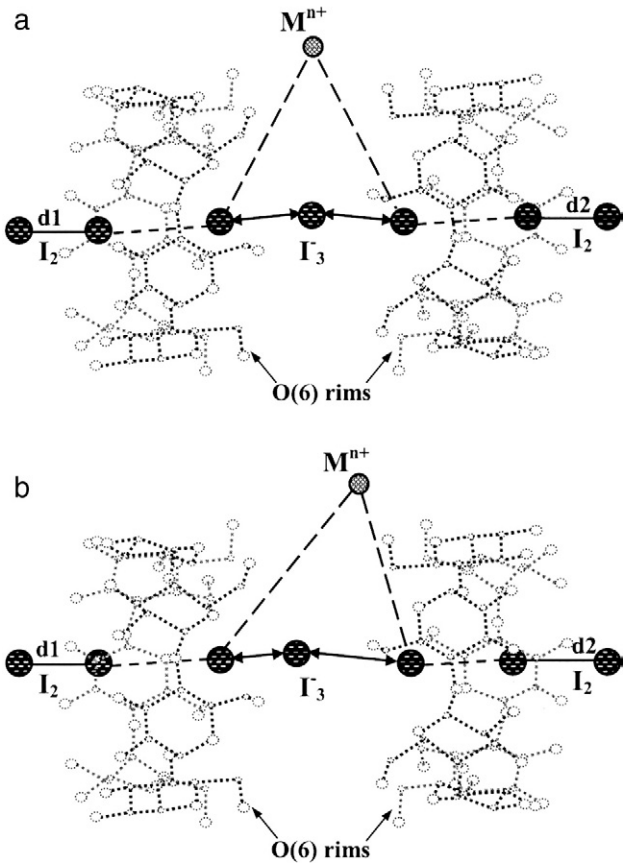

Fig. 1. $M^{n+}\cdots I^-_3$ interactions in the β-CD polyiodide complexes whose metals present an ionic potential greater than ~1.50. The I_2 units of I^-_7 have become well-ordered (disorder–order transition) and the heptaiodide structure is viewed along the α-axis. (a) The metal ion (Sr^{2+}, Bi^{3+}) presents a face-on position relative to the I^-_3 ion attenuating the symmetric charge-transfer interaction $I_2 \leftarrow I^-_3 \rightarrow I_2$ ($d1 = d2 < 2.77$ Å). (b) The metal ion (Li^+, Cd^{2+}, V^{3+}) presents a side-on position relative to the I^-_3 ion causing a non-symmetric charge-transfer interaction $I_2 \leftarrow I^-_3 \longrightarrow I_2$ ($d1 < d2 = 2.77$ Å).

very fine reddish-brown thin needles of β-Te were grown, separated in a Buchner filter and dried in air. For β-Bi the same synthetic route has been employed using 1 g of β-CD, 0.45 g of bismuth iodide and 0.44 g of solid iodine as appropriate [13].

Simultaneous thermogravimetry (TGA) and differential thermal analysis (DTA) of β-Te were performed using a NETZSCH-STA 409 EP Controller TASC 414/3 (reference Al_2O_3). The sample (77 mg) was heated in the temperature range of 20–145 °C with a heating rate of 5 °C min^{-1}.

The experimental X-ray powder diffraction pattern of β-Te was obtained at room temperature with a Siemens D 5000 diffractometer using Cu Kα1 radiation ($\lambda = 1.54059$ Å) at 40 kV, 30 mA and graphite monochromator. The diffraction data were collected in the 2θ range of 5–55° with a constant step of 0.015° and a counting time of 11 s/step. The calculation of the simulated X-ray powder diffraction pattern of $(\beta\text{-CD})_2{\cdot}KI_7{\cdot}9H_2O$ [7] and the Rietveld refinement of the lattice parameters were performed by the computer program POWDER CELL 2.4 developed by Nolze and Kraus [17,18].

The Raman spectra of β-Te were obtained at 4 cm^{-1} resolution from 3500 cm^{-1} to 100 cm^{-1} with a data point interval of 1 cm^{-1} using a Perkin–Elmer NIR FT spectrometer (Spectrum GX II) equipped with an InGaAs detector. The laser power and spot (Nd: YAG at 1064 nm) were controlled to be constant at 50 mW during the measurements and 400 scans were accumulated. The polycrystalline sample was gradually heated from 30 to 120 °C, by raising the temperature in 10 °C increments in the range of 30–70 °C, in 5 °C increments in the range of 70–110 °C and in 10 °C increment in the range of 110–120 °C. The temperature variation was controlled with a Ventacon Winchester instrument equipped with a CALCOMMS 3300 autotune controller.

For the dielectric spectroscopy study, pressed pellets of powdered samples, 20 mm in diameter with thickness 0.95 mm for β-Bi and 0.99 mm for β-Te, were prepared with a pressure pump (Riken Power model P-1B) at room temperature. Two platinum foil electrodes were pressed at the same time with the sample. The pellet was then loaded in a temperature-controlled chamber, between two brass rods accompanied by a compression spring. A K-type thermocouple was kept close to the sample, and the whole cell was kept under N_2 atmosphere. The dielectric measurements were taken using a low frequency (0–100 kHz) dynamic signal analyser (DSA-Hewlett-Packard 3561A), in the temperature range of 140–425 K, operating at both frequency and time domains which is capable of measuring amplitude and phase accurately relative to a trigger signal. The data can be transferred to a PC through a HP 82335 Interface Bus (IEEE-488), where it can be stored and analyzed by a software program (*2plt*-1996). An analytical description of the process is given in previous articles [6,8].The imaginary and real parts of either impedance or dielectric constant versus frequency and temperature can be calculated and plotted.

The differential scanning calorimetry (DSC) method (Perkin–Elmer DSC-4 instrument) was used with a thermal analysis data station (TADS) system for all calorimetric measurements. Known weights (12–14 mg) of β-Bi and β-Te were sealed into aluminum pans and then heated from 0 up to 150 °C, with a heating rate of 10 °C min^{-1}, in a dynamic nitrogen atmosphere. The instrument was calibrated using indium at the same scanning rate as the samples.

3. Results

3.1. Characterization of the β-cyclodextrin polyiodide complex with Te^{4+}

3.1.1. Thermal analysis

The thermogravimetric analysis (TGA) and differential thermal analysis (DTA) curves (5 °C min^{-1}) of β-Te are shown in Fig. 2. The number of water molecules per dimer was calculated from the weight loss in the temperature range of ~55–127 °C, where the dehydration process takes place. The result is in agreement with ~17 water molecules per β-cyclodextrin dimer. Thus, the general composition is $(\beta\text{-CD})_2{\cdot}TeI_7{\cdot}17H_2O$. In the case of β-Bi the number of water molecules per dimer has been previously determined [13] and its general composition is $(\beta\text{-CD})_2{\cdot}BiI_7{\cdot}17H_2O$.

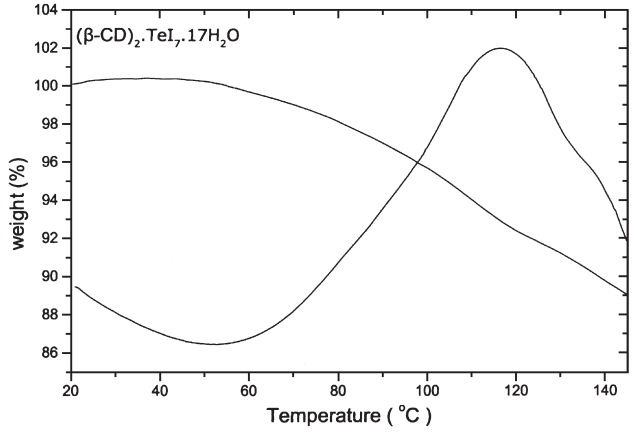

Fig. 2. Simultaneous thermogravimetry (TGA) and differential thermal analysis (DTA) of $(\beta\text{-CD})_2\cdot TeI_7\cdot 17H_2O$, with a heating rate of 5 °C·min^{-1}.

3.1.2. X-ray powder diffraction and Rietveld analysis

A few grams of polycrystalline β-Te were finely hand-pulverized in order to reduce the greater volume fraction of certain crystal orientations (texture) in the sample. We collected the experimental XRD pattern at room temperature covering the 5–55° 2θ range, in order to perform a Rietveld refinement of the lattice parameters. Fig. 3 shows the experimental X-ray powder diffraction pattern of β-Te and the Rietveld refinement of this profile (POWDER CELL 2.4 software) with the monoclinic $P2_1$ structure of $(\beta\text{-CD})_2\cdot KI_7\cdot 9H_2O$ [7] : R_p=6.88%, R_{wp}=9.86%, R_{exp}=6.98% and χ^2=1.995. We obtained the following lattice parameters a=19.5392(2) Å, b=24.4130(0) Å, c=15.8841 (5) Å and β=109.953(0)°, which differ by less than 1% from those values reported by Betzel et al. [7]. We note that some experimental peak intensities at room temperature vary from those calculated, mainly due to the fact that the iodine atoms of the heptaiodides present fractional coordinates and bond lengths that differ from the corresponding ones in the single crystal of β-K. This structural change becomes obvious from the following Raman spectroscopic results. Additionally, thermal analysis showed that β-Te presents a greater degree of hydration per dimer (17 H_2O) than that of β-K (9 H_2O) indicating that the water molecules of these systems are not expected to display equivalent positions and identical local

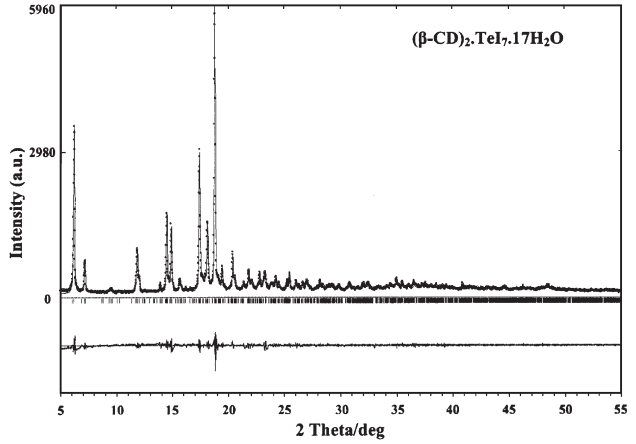

Fig. 3. Rietveld refinement pattern of $(\beta\text{-CD})_2\cdot TeI_7\cdot 17H_2O$. Black circles: experimental pattern, solid line: refined model. The curve at the bottom is the difference between the observed and calculated intensities in the same scale. Black vertical lines indicate the positions of the allowed reflections.

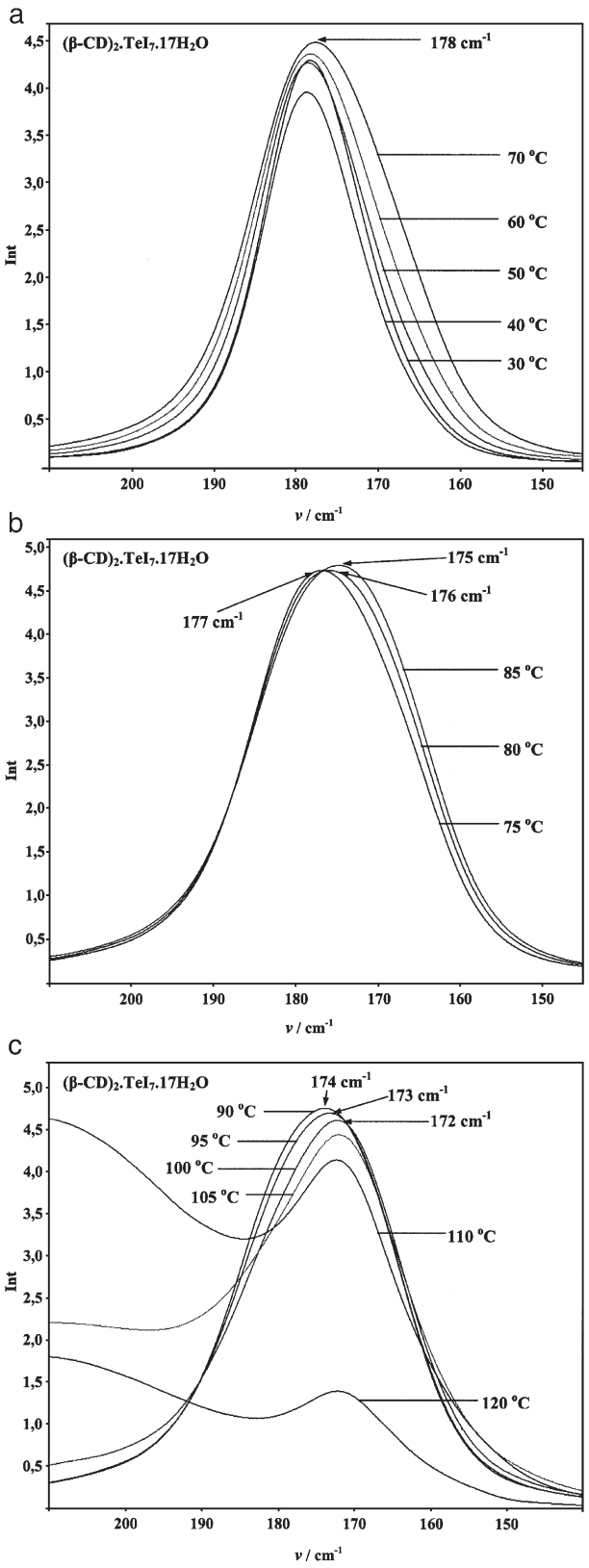

Fig. 4. Raman spectra of $(\beta\text{-CD})_2\cdot TeI_7\cdot 17H_2O$ during heating, in the temperature ranges of (a) 30–70 °C, (b) 75–85 °C, and (c) 90–120 °C.

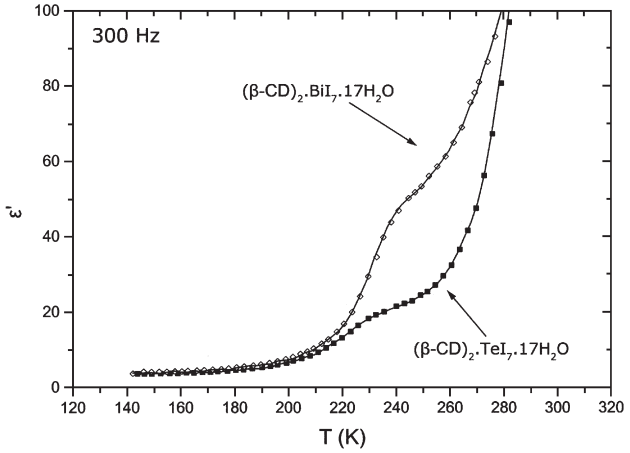

Fig. 5. Temperature dependence of the real (ε′) part of the dielectric constant of $(\beta\text{-CD})_2{\cdot}TeI_7{\cdot}17H_2O$ and $(\beta\text{-CD})_2{\cdot}BiI_7{\cdot}17H_2O$ at 300 Hz.

environments in the interstices. Finally, the total absence of any hump (indicative of amorphous material) proves the purity of the synthesized inclusion complex (single phase). The X-ray powder diffraction study of β-Bi [13] has also revealed a monoclinic $P2_1$ crystalline form (isomorphous to β-K [7]) of high purity.

3.1.3. Raman spectroscopy

The Raman spectra of β-Te during the heating process in the range of 30–120 °C are shown in Fig. 4a–c. Initially, at 30 °C there is one strong band at 178 cm^{-1} with an intensity of 4.29. At 40 °C the intensity decreases to 3.95, whereas as the sample is heated up to 70 °C, it gradually increases to the value of 4.48. At the temperatures of 75, 80 and 85 °C the initial band is shifted to the frequencies of 177, 176 and 175 cm^{-1}, respectively. At 90 °C there is a band at 174 cm^{-1} with an intensity of 4.75 which is shifted to 173 cm^{-1} at 95 °C presenting an intensity of 4.69. Finally, in the range of 100–120 °C a band at 172 cm^{-1} is observed with gradually decreased intensity.

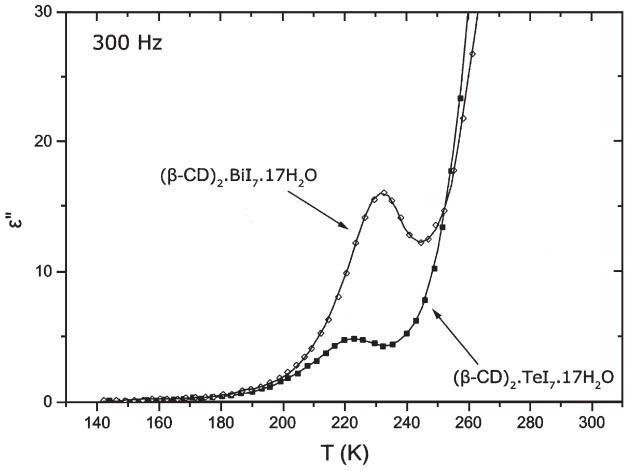

Fig. 6. Temperature dependence of the imaginary (ε″) part of the dielectric constant of $(\beta\text{-CD})_2{\cdot}TeI_7{\cdot}17H_2O$ and $(\beta\text{-CD})_2{\cdot}BiI_7{\cdot}17H_2O$ at 300 Hz.

3.2. Dielectric spectroscopy and differential scanning calorimetry (DSC) of the β-cyclodextrin polyiodide complexes with Te^{4+} and Bi^{3+}

3.2.1. Temperature dependence of the dielectric constant (ε′, ε″)

The temperature dependences of the real part ε′ and the imaginary part ε″ of the dielectric constant over the temperature range of 140–290 K, at a frequency of 300 Hz, are shown in Figs. 5 and 6 for both β-Te and β-Bi.

The real part ε′of β-Te, increases in a single and clear sigmoid fashion from 3.7 at 144 K to 22.3 at 243 K with an inflection point of 13.2 at 219.9 K. Above 243 K, ε′ increases rapidly to the value of 97 at 282.2 K. The ε″(*T*) plot shows, a single bell-shaped curve with a peak value of 4.8 at 223.1 K and an abrupt increment above 240 K, to the value of 23.3 at 257.5 K. By increasing the frequency of the applied field to 1 kHz, the single sigmoid of the ε′(*T*) plot and the bell-shaped curve of the ε″(*T*) plot, remain distinguishable. The same qualitative picture is observed for higher fixed frequencies in the range of 10–100 kHz.

In the case of β-Bi, ε′ increases in a very high sigmoid fashion from 3.7 at 142.2 K to 53.3 at 249.4 K with an inflection point of 29.4 at 229.6 K. Above 249.4 K, ε′ increases rapidly to the value of 93.1 at 276.9 K. The imaginary part ε″ presents a

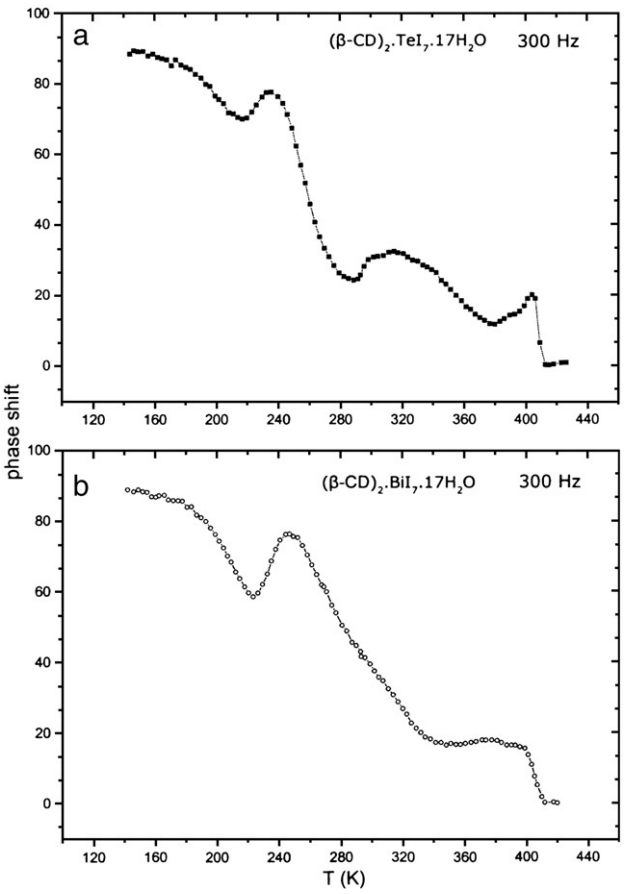

Fig. 7. Temperature dependence of the phase shift (φ) of (a) $(\beta\text{-CD})_2{\cdot}TeI_7{\cdot}17H_2O$ and (b) $(\beta\text{-CD})_2{\cdot}BiI_7{\cdot}17H_2O$, at 300 Hz.

sharp bell-shaped curve with peak value $\varepsilon'' = 16$ at 232.7 K and an abrupt increase above 247 K to the value of 26.7 at 261.4 K. By increasing the frequency of the applied field to 1 kHz the sigmoid in the $\varepsilon'(T)$ plot and the bell-shaped curve in the $\varepsilon''(T)$ plot remain distinguishable. At higher frequencies (10–100 kHz) the same behaviour is observed.

3.2.2. Temperature dependence of the phase shift (φ)

The phase shift φ of β-Te at a fixed frequency of 300 Hz (Fig. 7a), presents three topical minimum values over the temperature range of 140–425 K. Specifically, it drops from 88.4° at 144 K to a minimum value of 69.9° at 216.8 K, then it increases to 77.6° at 235.5 K and decreases rapidly to 24.2° at 288.7 K; then it increases to 32.4° at 314.6 K, decreases to a minimum value of 11.7° at 379.7 K and increases again to 20.1° at 404 K. Finally, at $T > 404$ K it decreases to a plateau-like region with a minimum value of 0.3° at 412.5 K. At higher fixed frequencies similar behaviour is observed.

The phase shift φ of β-Bi at a fixed frequency of 300 Hz (Fig. 7b) over the range of 140–425 K, presents one topical minimum value at $T < 250$ K and an abrupt decrease at $T > 250$ K. Specifically, it drops from 88.8° at 142.2 K to a minimum value of 58.6° at 223.6 K, then it increases to 76.3° at 247 K and decreases to a plateau-like region with a minimum value of 16.6° at 348 K; then it increases again to 18.1° at 377.4 K and drops to 16.5° at 392.7 K. Finally, at $T > 398.9$ K, it decreases to 0.1° at 420 K. At higher fixed frequencies the topical minimum and the plateau-like region remain clearly distinguishable.

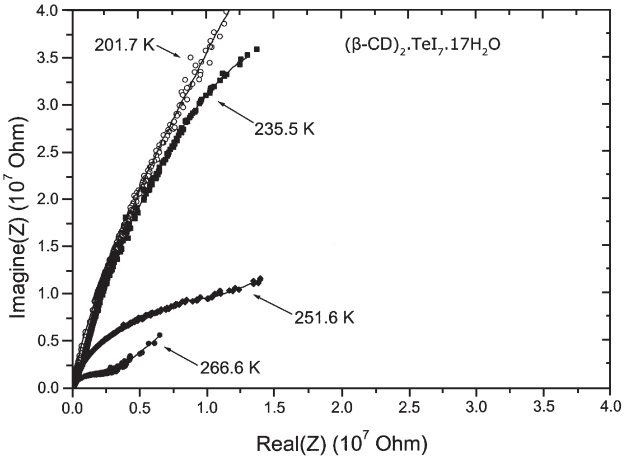

Fig. 9. Impedance diagram of $(\beta\text{-CD})_2{\cdot}TeI_7{\cdot}17H_2O$ in the temperature range of 201.7–266.6 K.

3.2.3. Temperature dependence of the ac-conductivity ($\ln\sigma(1/T)$)

The temperature variation of the ac-conductivity ($\ln\sigma$ *vs.* $1/T$) of β-Te during the heating process, under an applied frequency of 300 Hz is shown in Fig. 8a. This plot shows the extended sigmoid curve (a) at $10^3/T > 4.12$ K^{-1} and the linear parts (b) and (c) in the temperature range of 2.90 K^{-1} $< 10^3/T < 4.12$ K^{-1}. In the range of 2.51 K^{-1} $< 10^3/T < 2.90$ K^{-1} the conductivity deviates from the exponential increment, whereas at $10^3/T < 2.51$ K^{-1} it increases abruptly (linear part (d)), taking a maximum value at $10^3/T = 2.41$ K^{-1} and then decreasing up to $10^3/T = 2.35$ K^{-1}. Concerning β-Bi the ac-conductivity (Fig. 8b) presents the extended sigmoid curve (a) at $10^3/T > 4.05$ K^{-1} and the linear parts (b), (c) and (d) in the temperature range of 2.51 K^{-1} $< 10^3/T < 4.05$ K^{-1}. Finally, at $10^3/T < 2.51$ K^{-1} there is an abrupt

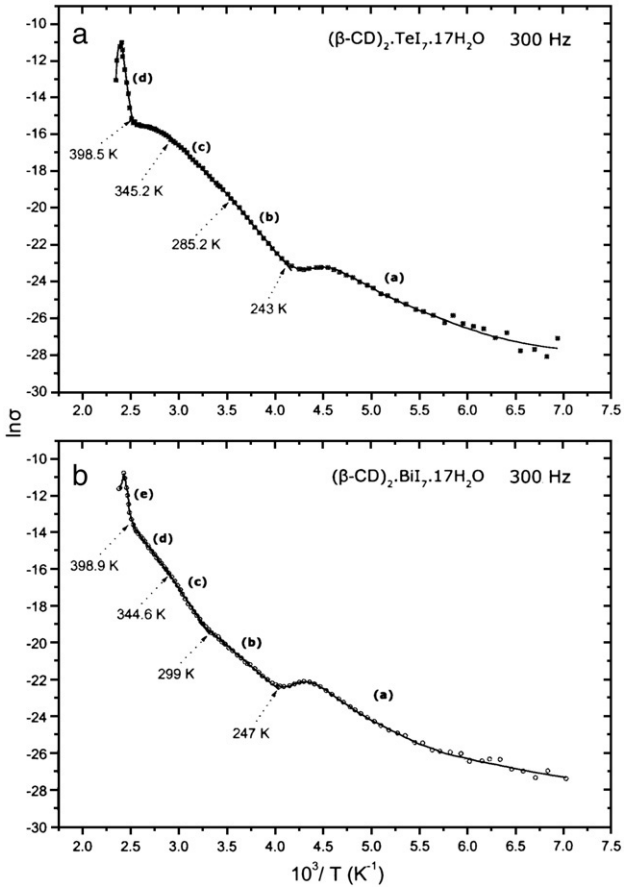

Fig. 8. Temperature dependence of the ac-conductivity ($\ln\sigma$ *vs.* $1/T$) of (a) $(\beta\text{-CD})_2{\cdot}TeI_7{\cdot}17H_2O$ and (b) $(\beta\text{-CD})_2{\cdot}BiI_7{\cdot}17H_2O$, at 300 Hz.

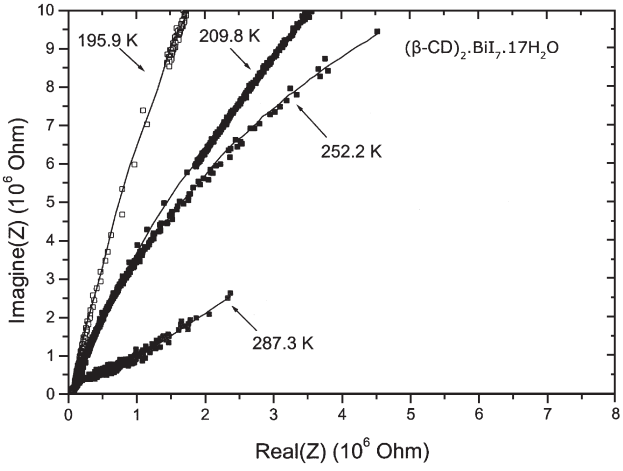

Fig. 10. Impedance diagram of $(\beta\text{-CD})_2{\cdot}BiI_7{\cdot}17H_2O$ in the temperature range of 195.9–287.3 K.

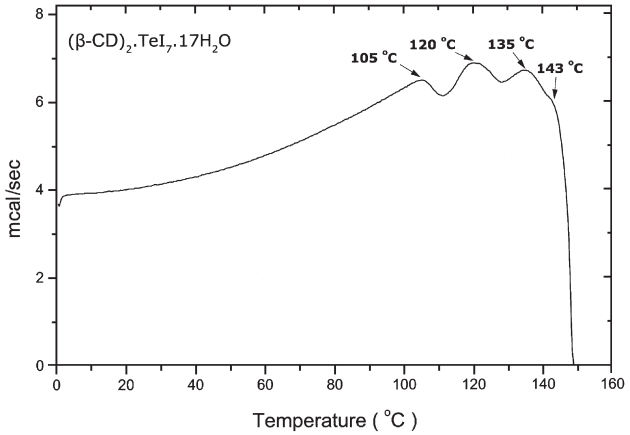

Fig. 11. DSC thermogram of $(\beta\text{-CD})_2{\cdot}TeI_7{\cdot}17H_2O$ with a heating rate of 10 °C·min^{-1}.

increase of the ac-conductivity (linear part (e)) up to $10^3/T=2.43$ K^{-1} and then a decrease up to $10^3/T=2.38$ K^{-1}.

3.2.4. Impedance diagrams

The impedance diagram ImZ *vs*. ReZ (0–100 kHz) of β-Te in the temperature range of 201.7–266.6 K (Fig. 9), presents circular arcs whose radii continuously decrease. The generated linear segment in the low frequency region at ~251.6 K, becomes well-distinguishable at 266.6 K. The impedance diagram of β-Bi in the temperature range of 195.9–287.3 K (Fig. 10), shows circular arcs with gradually decreased radii. At ~287.3 K a linear segment is generated in the low frequency region.

3.2.5. DSC thermograms

The DSC trace of β-Te (Fig. 11) recorded with a scan rate of 10 °C min^{-1} shows three broad endothermic peaks at the temperatures of 105, 120 and 135 °C and a shoulder at 143 °C. The DSC trace of β-Bi (Fig. 12) also recorded with a scan rate of 10 °C min^{-1} shows a slab shoulder at 101 °C, two broad endothermic peaks at the temperatures of 118 and 134 °C and a sharp-double endothermic peak with temperatures 146 and 148 °C. At temperatures higher than ~148 °C, both traces present downward baselines which indicate the decomposition of the samples.

4. Discussion

In the temperature range of 140–250 K, both β-Te and β-Bi exhibit dielectric relaxation properties which significantly differ from those of the previously investigated β-CD heptaiodide complexes with various metal ions [8–11]. More explicitly, in the case of β-Ba, β-Cd, β-Li, β-K and β-Cs the corresponding $\varepsilon'(T)$ variations increased with temperature in a step-like form of low height ($6 \le \Delta\varepsilon' \le 8.4$) presenting inflection points that were located at approximately 200 K. Furthermore, their $\varepsilon''(T)$ and $\varphi(T)$ variations displayed hardly distinguishable bell-shaped curves ($0.7 \le \varepsilon''_{max} \le 1.4$ at ~200 K) and topical minima of low depth ($81.7° \le \varphi_{min} \le 82.7°$ at ~200 K), respectively. These experimental data indicated that during the following order–disorder transition (T_{trans}=~200 K):

$$\underset{\text{(normal H−bonds)}}{O\text{—}H\cdots O\text{—}H} \rightarrow O\text{—}\underset{\text{(flip−flop H−bonds)}}{(1/2H)\cdots(1/2H)}\text{—}O \qquad (1)$$

very few normal hydrogen bonds were transformed into those of the flip-flop type resulting in a rather limited flip-flop hydrogen-bonding network along with small changes in the polarization and the ac-conductance of these polycrystalline specimens. In the present study the ε'values of β-Te increase in a step-like form of considerable height ($\Delta\varepsilon'=18.6$), whereas the $\varepsilon''(T)$ and $\varphi(T)$ functions present a well-distinguishable bell-shaped curve ($\varepsilon''_{max}=4.8$) and a clear topical minimum ($\varphi_{min}=69.9°$), respectively. Therefore, it becomes apparent that as the temperature is raised an important percentage of normal hydrogen bonds is transformed into flip-flop ones in the crystal lattice of β-Te (T_{trans}=216.8 K according to Fig. 7a), revealing a more extensive flip-flop hydrogen-bonding network than those of the aforementioned β-CD polyiodide complexes. Even though these results appear sufficiently sound, the β-Bi system is the one with the most peculiar dielectric behaviour at $T<250$ K. More specifically, the ε' values increase in an extremely high step-like form ($\Delta\varepsilon'=49.6$), while the $\varepsilon''(T)$ variation presents a very sharp bell-shaped curve ($\varepsilon''_{max}=16$) and finally the $\varphi(T)$ variation displays a topical minimum of remarkable depth ($\varphi_{min}=58.6°$). These findings suggest that during the heating process the greatest percentage of normal hydrogen bonds is transformed into flip-flop ones in the crystal lattice of β-Bi (T_{trans}=223.6 K according to Fig. 7b) causing tremendous changes in the polarization and the ac-conductance. Thus, the existing flip-flop hydrogen-bonding network in β-Bi is of a much higher density than the corresponding one in β-Te, indicating a more complicated structural feature.

At $T>250$ K, the conductance of the two systems increases rapidly resulting in very high values of ε' and ε'' that have no significance in the conventional dielectric sense [19]. For this reason, we focus on the temperature dependence of the ac-conductivity which clearly depicts all the different charge-transport phenomena that take place in the range of 140–425 K. In the lnσ

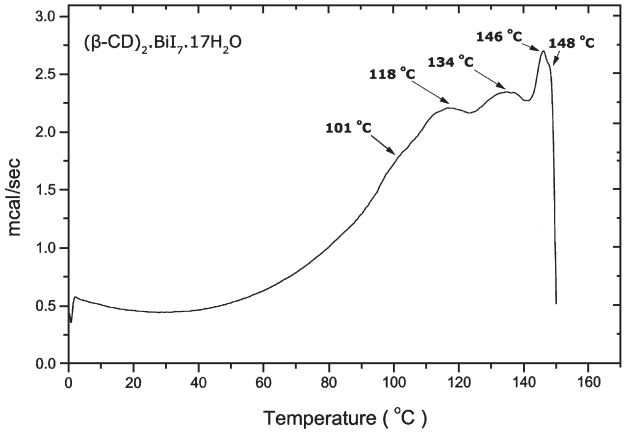

Fig. 12. DSC thermogram of $(\beta\text{-CD})_2{\cdot}BiI_7{\cdot}17H_2O$ with a heating rate of 10 °C·min^{-1}.

versus $1/T$ plot of β-Te (Fig. 8a) the extended sigmoid (a) at $T<243$ K, is caused by the order–disorder transition (1). The linear part (b) in the range of 243–285.2 K exhibits an Arrhenius behaviour according to the semiconduction equation $\sigma=\sigma_o\exp(-E_a/kT)$, with activation energy $E_a=0.54$ eV. This exponential variation is a result of the continuous transformation:

$$(H_2O)_{\text{tightly bound}} \rightarrow (H_2O)_{\text{easily movable}} \quad (2)$$

and of the tellurium ions' contribution. The interconnection between these two mechanisms becomes evident from the impedance diagram of Fig. 9. As the temperature is raised, the radii of the circular arcs decrease since the thermally activated processes (1) and (2) involve a gradual increment of the reorientated dipoles in the crystals and a progressive reduction of the grain interior impedance. The generated linear segment in the low frequency region at ~251.6 K indicates the onset of space charge in the material [20–22]. This effect is directly related to the released Te^{4+} ions which oscillate with the frequency of the applied field contributing to the ac-conductivity along with a chemical exchange of H^+ in the water network described as Grotthuss mechanism [23–25]. The rapid increase of σ up to 285.2 K, is consistent with the abrupt decrease of φ up to 288.7 K (Fig. 7a), revealing that a great number of water molecules have been transformed into easily movable ones.

The linear part (c) in the range of 285.2–345.2 K also follows the Arrhenius law with $E_a=0.46$ eV. This activation energy is lower than that of the linear part (b) because the transformation (2) of the remaining tightly bound water molecules is strongly affected by the simultaneous dehydration process. More explicitly, at $T>345.2$ K, the ac-conductivity deviates from the above exponential behaviour even though the aforementioned transformation continues to take place up to 379.7 K according to the $\varphi(T)$ plot (Fig. 7a). This deviation is due to the dehydration process which has a significant impact on the electrical properties leading to both the breakdown of the water network and the attenuation of the proton conduction. Furthermore, the continuous removal of the water molecules from the crystal lattice minimizes the contribution of the tellurium ions that act as localized charges. Finally, the abrupt increase of the ac-conductivity at $T>398.5$ K, is caused by the sublimation of iodine which provides conduction paths along the polyiodide chains resulting in strong electron interactions between the neighboring heptaiodide ions [8–12]. These experimental data are consistent with those obtained from the differential scanning calorimetry method. The endothermic peaks at 378 K (105 °C) and 393 K (120 °C) (Fig. 11) are directly related to the two kinds of water molecules in β-Te. More specifically, the former peak corresponds to the evaporation of the H_2O molecules that have been transformed into the easily movable state earlier (at lower temperatures) than those whose evaporation is responsible for the latter peak. The third endothermic peak at 408 K (135 °C) is due to the sublimation of iodine that involves the gradual decomposition of the I^-_7 ions displayed by the following scheme:

$$I_2 \cdot I^-_3 \cdot I_2 \rightarrow I^-_3 + 2I_2 \quad (3)$$

The shoulder at 416 K (143 °C) is interpreted in terms of the decomposition of I^-_3 ions which succeeds Eq. (3) to form I_2 and I^-:

$$I^-_3 \rightarrow I_2 + I^- \quad (4)$$

The effusion of the sublimed iodine molecules at higher temperatures causes the rupture of the grain boundaries which is responsible for the downward baseline above ~421 K (148 °C) in the DSC trace. This procedure should not be related to the decomposition of the β-CD molecules since the latter begins at $T>523$ K [26,27].

In the $\ln\sigma$ versus $1/T$ plot of β-Bi (Fig. 8b) the very high sigmoid curve (a) at $T<247$ K, is attributed to the order–disorder transition (1) that takes place to a great extent. The linear part (b) in the range of 247–299 K presents an Arrhenius behaviour with $E_a=0.38$ eV as a consequence of the continuous transformation (2). For this reason the phase shift φ drops abruptly at $T>247$ K (Fig. 7b). The linear part (c) in the range of 299–344.6 K displays a greater activation energy ($E_a=0.68$ eV) than that of (b) due to the release of bismuth ions which increases the number of the mobile charge carriers in the sample. This can be viewed in the impedance diagram (Fig. 10) where the gradually decreased radii of the circular arcs during heating are a result of (1) and (2), while the linear response in the low frequency region at ~287.3 K implies the transport of Bi^{3+} ions. The linear part (d) in the range of 344.6–398.9 K, exhibits an activation energy of 0.58 eV which is lower than the corresponding one of (c). That happens because the dehydration process progressively reduces the number of the reorientated H_2O dipoles in the crystal lattice. This is also confirmed by the DSC peaks (Fig. 12) at 374 K (101 °C) and 391 K (118 °C) which are related to the gradual removal of the two kinds of water molecules in β-Bi. The third endothermic peak at 407 K (134 °C) corresponds to the sublimation of iodine (scheme (3)) that results in the rapid increment of the ac-conductivity at $T>398.9$ K. Finally, the sharp-double endothermic peak with temperatures 419 and 421 K (146 and 148 °C) indicates that during the decomposition of I^-_3 ions the associated enthalpy change ΔH is greater than the one in the case of β-Te (small DSC shoulder at 143 °C). This suggests fundamental differences in the local environments of the triiodides in each system. These differences can be explained by taking into consideration the Raman spectroscopic results of β-Bi and β-Te complexes.

The previously investigated Raman spectra of β-Bi exhibited a gradual shift of the initial band at 178 cm^{-1} to the final single frequency of 172 cm^{-1} as the temperature was raised (30–130 °C), indicating a symmetric charge-transfer interaction $I_2 \leftarrow I^-_3 \rightarrow I_2$ and a face-on position of Bi^{3+} relative to the I^-_3 ion [13]. In the present work, the temperature-dependent (30–120 °C) Raman spectra of β-Te display exactly the same band shift (178 → 172 cm^{-1}) which is also consistent with a face-on position of Te^{4+} relative to the triiodide (Fig. 1a). The common final frequency of 172 cm^{-1} reveals that the disordered I_2 units of both β-Te and β-Bi present an identical elongation with temperature, implying that the e^- donor ability of I^-_3 is attenuated to the same extent by the Te^{4+} and Bi^{3+} ions. This fact seems rather peculiar since the ionic potential of Bi^{3+} (3.26) is lower than that of Te^{4+} (4.49). The most plausible rationalization of this discrepancy is that apart from the Bi^{3+} ion the enormously disordered hydrogen-bonding network plays a key role

in limiting the Lewis base character of I^-_3. Crystallographic and ab initio studies have shown that the major part of the electron density of I^-_3 is localized on its terminal I atoms rendering them excellent e^- donors [28–33]. We believe that these negatively charged atoms participate in the high density flip-flop H-bonding network of β-Bi, by closing one or more flip-flop circular rings [1–3]. According to this point of view, each one of the outer I atoms is expected to accept a certain number of dynamically disordered hydrogen atoms H that belong to the vicinal O(6) hydroxyl groups. The possibility of such a stuctural feature is strengthened by the sharp-double DSC peak (146 and 148 °C) in Fig. 12, which can be interpreted in terms of the I^-_3 decomposition (146 °C) resulting in the subsequent rupture of the local O(6)–H···I^-_3 interactions (148 °C). At this point, we avoid any further discussion since only a detailed neutron-diffraction analysis by an experienced crystallographer can provide a thorough description of the complicated flip-flop arrangements and the relevant intermolecular interactions. However, the combination of dielectric relaxation, Raman spectroscopy and thermal analysis suggests that in β-Bi the e^- donor ability of the triiodide is affected by both the bismuth ion and the existing flip-flop network. A relatively comparable scheme has been reported by Peralta–Inga and co-workers for α-cellobiose·2NaI·2H_2O where the I^- ions act as long H-bonding chain terminators accepting several hydrogen bonds as well as sodium ions [34]. In the case of β-Te the symmetric charge-transfer interaction $I_2 \leftarrow I^-_3 \rightarrow I_2$ is mainly attenuated by the Te^{4+} since the negatively charged I atoms of I^-_3 do not seem to be involved in the corresponding flip-flop network.

5. Concluding remarks

The present study reveals that at $T<250$ K, both β-Te and β-Bi display dielectric properties which significantly differ from those of the previously investigated β-CD heptaiodide complexes with various metal ions. In β-Te an important percentage of normal hydrogen bonds is transformed into those of flip-flop type ($T_{trans}=216.8$ K), resulting in a quite extensive flip-flop hydrogen-bonding network. However, in β-Bi the greatest percentage of normal hydrogen bonds is transformed into flip-flop ones ($T_{trans}=223.6$ K), producing a flip-flop hydrogen-bonding network of a much higher density than that of β-Te. At $T>250$ K, the ac-conductivity of these systems presents an Arrhenius increment due to the continuous transformation $(H_2O)_{tightly\ bound} \rightarrow (H_2O)_{easily\ movable}$ and the contribution of the released metal ions via the water network. During the dehydration process there are deviations (lower increasing rate) from the above exponential variation since the gradual breakdown of the water network attenuates the proton conduction and turns the metal ions into localized charges. At $T>398.5$ K the ac-conductivity of β-Te and β-Bi increases abruptly as a result of the sublimation of iodine which provides conduction paths along the neighboring heptaiodide ions. All the above were also confirmed by the use of differential scanning calorimetry.

The previously investigated Raman spectra of β-Bi exhibited a gradual shift of the initial band at 178 cm^{-1} to the final single frequency of 172 cm^{-1} as the temperature was raised. In the present case the temperature-dependent Raman spectra of β-Te display exactly the same band shift. The common final frequency of 172 cm^{-1} reveals that the e^- donor ability of I^-_3 is attenuated to the same extent in both systems even though the ionic potential of Bi^{3+} (3.26) is lower than that of Te^{4+} (4.49). This fact implies that apart from the Bi^{3+} ion the high density flip-flop hydrogen-bonding network of β-Bi plays a key role in limiting the Lewis base character of I^-_3.

Acknowledgements

This work was carried out in partial fulfillment of the requirements for V.G.C's Ph.D. Thesis. It was partly supported by Grant No. 70/4/3347SARG, NKUA. We are grateful to Professor K. Viras for his assistance in conducting the Raman spectra and calorimetric measurements.

References

[1] W. Saenger, C. Betzel, B. Hingerty, G.M. Brown, Nature 296 (1982) 581.
[2] C. Betzel, W. Saenger, B.E. Hingerty, G.M. Brown, J. Am. Chem. Soc. 106 (1984) 7545.
[3] T. Steiner, S.A. Mason, W. Saenger, J. Am. Chem. Soc. 113 (1991) 5676.
[4] V. Zabel, W. Saenger, S.A. Mason, J. Am. Chem. Soc. 108 (1986) 3664.
[5] T. Fujiwara, M. Yamazaki, Y. Tomizu, R. Tokuoka, K. Tomita, T. Matsuo, H. Suga, W. Saenger, Nippon Kagaku Kaishi 2 (1983) 181.
[6] J.C. Papaioannou, N.D. Papadimitropoulos, I.M. Mavridis, Mol. Phys. 97 (1999) 611.
[7] C. Betzel, B. Hingerty, M. Noltemeyer, G. Weber, W. Saenger, J.A. Hamilton, J.Inclusion Phenom. Macrocyclic Chem. 1 (1983) 181.
[8] V.G. Charalampopoulos, J.C. Papaioannou, Mol. Phys. 103 (2005) 2621.
[9] V.G. Charalampopoulos, J.C. Papaioannou, H.S. Karayianni, Solid State Sci. 8 (2006) 97.
[10] J.C. Papaioannou, Mol. Phys. 102 (2004) 95.
[11] J.C. Papaioannou, V.G. Charalampopoulos, P. Xynogalas, K. Viras, J. Phys. Chem. Solids 67 (2006) 1379.
[12] A. Oza, Cryst. Res. Technol. 19 (1984) 697.
[13] V.G. Charalampopoulos, J.C. Papaioannou, G. Kakali, H.S. Karayianni, Carbohydr. Res. 343 (2008) 489.
[14] P. Deplano, F.A. Devillanova, J.R. Ferraro, F. Isaia, V. Lippolis, M.L. Mercuri, Appl. Spectrosc. 46 (1992) 1625.
[15] F. Demartin, P. Deplano, F.A. Devillanova, F. Isaia, V. Lippolis, G. Verani, Inorg. Chem. 32 (1993) 3694.
[16] L.B. Railsback, Geology 31 (2003) 737.
[17] W. Kraus, G. Nolze, J. Appl. Crystallogr. 29 (1996) 301.
[18] G. Nolze, W. Kraus, Powder Diffr. 13 (1998) 256.
[19] A.R. West, Solid State Chemistry and its applications, Wiley, 1984, p. 535.
[20] A.K. Jonscher, J. Mater. Sci. 13 (1978) 553.
[21] J.R. Macdonald, Impedance Spectroscopy, Wiley, New York, 1987, p. 252.
[22] V.G. Charalampopoulos, J.C. Papaioannou, Carbohydr. Res. 342 (2007) 2075.
[23] C.J.T. de Grotthuss, Ann. Chim. 58 (1806) 54.
[24] N. Agmon, Chem. Phys. Lett. 244 (1995) 456.
[25] B.V. Merinov, Solid State Ionics 84 (1996) 89.
[26] G. Bettinetti, Cs. Novak, M. Sorrenti, J. Therm. Anal. Calorim. 68 (2002) 517.
[27] Y.-A. Gao, Z.-H. Li, J.-M. Du, B.-X. Han, G.-Z. Li, W.-G. Hou, D. Shen, L.-Q. Zheng, G.-Y. Zhang, Chem. Eur. J. 11 (2005) 5875.
[28] J. Rusnink, S. Swen-Walstra, T. Migchelsen, Acta Cryst. B28 (1972) 1331.
[29] J.J. Novoa, F. Mota, S. Alvarez, J. Phys. Chem. 92 (1988) 6561.
[30] Z. Lin, M.B. Hall, Polyhedron 12 (1993) 1499.
[31] G.A. Landrum, N. Goldberg, R. Hoffmann, J. Chem. Soc. Dalton Trans. (1997) 3605.
[32] P.H. Svensson, L. Kloo, J. Chem. Soc. Dalton Trans. (2000) 2449.
[33] P.H. Svensson, L. Kloo, Chem. Rev. 103 (2003) 1649.
[34] Z. Peralta-Inga, G.P. Johnson, M.K. Dowd, J.A. Rendleman, E.D. Stevens, A.D. French, Carbohydr. Res. 337 (2002) 851.